

# Analyst

Accepted Manuscript



This is an *Accepted Manuscript*, which has been through the Royal Society of Chemistry peer review process and has been accepted for publication.

*Accepted Manuscripts* are published online shortly after acceptance, before technical editing, formatting and proof reading. Using this free service, authors can make their results available to the community, in citable form, before we publish the edited article. We will replace this *Accepted Manuscript* with the edited and formatted *Advance Article* as soon as it is available.

You can find more information about *Accepted Manuscripts* in the [Information for Authors](#).

Please note that technical editing may introduce minor changes to the text and/or graphics, which may alter content. The journal's standard [Terms & Conditions](#) and the [Ethical guidelines](#) still apply. In no event shall the Royal Society of Chemistry be held responsible for any errors or omissions in this *Accepted Manuscript* or any consequences arising from the use of any information it contains.

1  
2  
3  
4  
5  
6  
7 **On-chip metal/polypyrrole quasi-reference electrodes for robust ISFET**  
8  
9  
10 **operation**  
11  
12

13  
14 Carlos Duarte-Guevara<sup>1,6</sup>, Vikhram V. Swaminathan<sup>2,6</sup>, Mark Burgess<sup>3</sup>, Bobby Reddy, Jr.<sup>6</sup>, Eric Salm<sup>6</sup>,  
15  
16 Yi-Shao Liu<sup>4</sup>, Joaquin Rodriguez-Lopez<sup>3</sup>, and Rashid Bashir<sup>5,6\*</sup>  
17  
18

19  
20  
21  
22 <sup>1</sup> Department of Electrical and Computer Engineering, University of Illinois at Urbana-Champaign,  
23  
24 306 N. Wright St., Urbana, IL 61801 USA  
25

26  
27 <sup>2</sup> Department of Mechanical Science and Engineering, University of Illinois at Urbana-Champaign,  
28  
29 1206 W. Green St., Urbana, 61801, IL, USA  
30

31  
32 <sup>3</sup> Department of Chemistry, University of Illinois at Urbana-Champaign, 505 South Mathews  
33  
34 Avenue, Urbana, IL 61801 USA  
35

36  
37 <sup>4</sup> Taiwan Semiconductor Manufacturing Company, 9 Creation Rd, Hsinchu Science Park,  
38  
39 Hsinchu, Taiwan 300-77, R.O.C. Hsinchu, Taiwan  
40

41  
42 <sup>5</sup> Department of Bioengineering, University of Illinois at Urbana-Champaign, 1270 Digital Computer  
43  
44 Laboratory, 1304 W. Springfield Ave., Urbana, IL 61801 USA  
45

46  
47 <sup>6</sup> Micro and Nanotechnology Lab, University of Illinois at Urbana-Champaign, 208 N. Wright St.,  
48  
49 Urbana, IL 61801 USA  
50

51  
52 \*Corresponding Author:

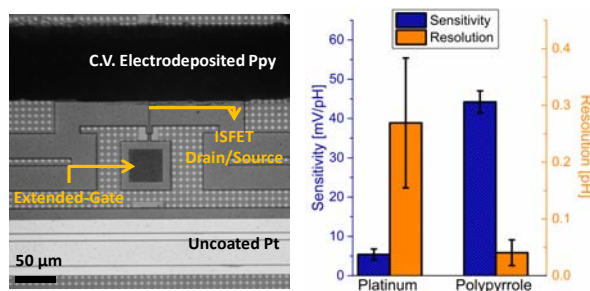
53  
54 Dr. Rashid Bashir

55  
56 1270 Digital Computer Laboratory, 1304 W. Springfield Ave., Urbana, IL 61801 USA

57  
58 Phone: 217-333-3097

59  
60 [rbashir@illinois.edu](mailto:rbashir@illinois.edu)

## Table of contents entry



Polypyrrole was deposited on metal electrodes with a cyclic voltammetry process to form robust on-chip quasi-reference electrodes. ISFETs operated with these electrodes are more sensitive and achieve better resolution.

**Abstract**

To operate an ion-sensitive field-effect transistor (ISFETs) it is necessary to set the electrolyte potential using a reference electrode. Conventional reference electrodes are bulky, fragile, and too big for applications where the electrolyte volume is small. Several researchers have proposed tackling this issue using a solid-state planar micro-reference electrode or a reference field-effect transistor. However, these approaches are limited by poor robustness, high cost, or complex integration with other microfabrication processes. Here we report a simple method to create robust on-chip quasi-reference electrodes by electrodepositing polypyrrole on micro-patterned metal leads. The electrodes were fabricated through the polymerization of pyrrole on patterned metals with a cyclic voltammetry process. Open circuit potential measurements were performed to characterize the polypyrrole electrode performance, demonstrating good stability ( $\pm 1$  mV), low drift ( $\sim 1$  mV/h), and reduced pH response (5 mV/pH). In addition, the polypyrrole deposition was repeated in microelectrodes made of different metals to test compatibility with standard complementary metal-oxide-semiconductor (CMOS) processes. Our results suggest that nickel, a metal commonly used in semiconductor foundries for silicide formation, is a good candidate to form the polypyrrole quasi-reference electrodes. Finally, the polypyrrole microelectrodes were used to operate foundry fabricated ISFETs. These experiments demonstrated that transistors biased with polypyrrole electrodes have pH sensitivity and resolution comparable to ones that are biased with standard reference electrodes. Therefore, the simple fabrication, high compatibility, and robust electrical performance make polypyrrole an ideal choice for the fabrication of outstanding microreference electrodes that enable robust and sensitive operation of multiple ISFET sensors on a chip.

**Keywords:** Ion-sensitive field-effect transistor, on-chip reference electrode, Polypyrrole, open circuit potential, cyclic voltammetry electrodeposition, CMOS-compatible.

## 1. Introduction

Challenges faced by the healthcare and regulatory industries are driving the development of new miniaturized biological sensors that promise to revolutionize diagnostics and screening methods.<sup>1,2</sup> The demand from these industries for higher quality biosensing with lower costs could be met by creating novel sensing systems with the ideal characteristics of portability, multiplexed analysis, low-cost, and automation.<sup>3,4</sup> At the fore-front of new approaches for biosensing are the field-effect transistor (FET) strategies for label free molecular and chemical detection.<sup>5,6</sup> Applying more than 50 years of development in the semiconductor industry to the diagnostics challenges could be the key to reducing the cost and complexity of biological assays while sustaining the required sensitivity and specificity.<sup>7</sup> Several researchers have explored this concept in the last decade improving methods and devices for FET-based biological sensing. Examples include the use of ion-sensitive field-effect transistors (ISFETs) to electrically monitor different biochemical processes,<sup>8,9</sup> modification of nanowire-FETs with capture molecules to detect the charge of a target analyte,<sup>10</sup> commercial use of highly multiplexed ISFET detection systems to perform fast and inexpensive DNA sequencing,<sup>11</sup> and development of theoretical/numerical frameworks for analysis and modeling of the FET structures.<sup>12</sup> The FET-based sensing technologies promise to fundamentally change strategies for detection of biological entities, and create a new generation of biosensing instruments.

One of the key challenges that has prevented the broad incorporation of ISFETs into biosensing systems is the practical limitation of the conventional reference electrode that is required to operate the transistors.<sup>13</sup> Commonly used Ag/AgCl reference electrodes are too big, fragile, and expensive for applications that use small volumes (e.g. droplets) or target portable/disposable devices.<sup>14</sup> To the replace common reference electrodes, various micro-fabricated electrodes have been reported in the past.<sup>15</sup> For example, a combination of thin-film metal deposition and agar gel saturated with KCl was used to mimic Ag/AgCl electrochemical referencing mechanisms on a

1  
2  
3  
4  
5  
6 miniature solid-state planar electrode.<sup>16,17</sup> Also, platinum has been treated with hydrogen gas,  
7  
8 Nafion, and perfluorosulfonic acid polymer, to create reference electrodes for miniaturized  
9  
10 electrochemical cells.<sup>18,19</sup> In addition, greater miniaturization has been achieved with microscopic  
11  
12 quasi-reference electrodes (a reference that does not have an established potential but varies  
13  
14 predictably under certain conditions)<sup>20</sup> that have been fabricated with iridium oxide<sup>21</sup> and with  
15  
16 polyvinyl chloride (PVC) as a passivation layer.<sup>22</sup> Despite good reported stability and reliability,  
17  
18 these miniaturized reference electrodes are undermined by complex and expensive fabrication  
19  
20 protocols that involve several micro-machining steps, complicated chemical processes, the use of  
21  
22 expensive precious metals and reagents, or incompatibility with other processes involved in silicon  
23  
24 transistor fabrication. Therefore, due to a combination of complexity, cost, and process  
25  
26 compatibility issues, it is unlikely that these previous approaches for miniaturization of reference  
27  
28 electrodes will be successful alternatives for referencing FET-based biosensors, especially when the  
29  
30 transistors are used for screening applications where multiple reactions are performed in a single  
31  
32 assay.  
33  
34

35  
36 In this paper, we report the simple fabrication of stable and pH insensitive on-chip quasi-reference  
37  
38 electrodes through the electrodeposition of polypyrrole (PPy) on patterned metals. The PPy coating  
39  
40 process involves cyclic voltammetry to polymerize pyrrole on a working metal electrode. The  
41  
42 process was originally described by Bard et al., on platinum and stainless steel wires<sup>23</sup> and has been  
43  
44 adopted by many others to create quasi-reference electrodes for electrochemical experiments with  
45  
46 small or localized volumes such as scanning electrochemical microscopy.<sup>24,25</sup> We used a similar  
47  
48 technique to create on-chip quasi-reference electrodes with photolithography patterned metals and  
49  
50 evaluated their robustness and pH stability using open circuit potential measurements. Our results  
51  
52 indicate that with the on-chip PPy electrodes random potential fluctuations are less than 1 mV, drift  
53  
54 is typically between 1-2 mV/h, and potential changes due to pH variations are normally below 5  
55  
56 mV/pH. Other results demonstrate that the PPy deposition process is compatible with CMOS  
57  
58  
59  
60

1  
2  
3  
4  
5  
6 processes, and that operation of ISFETs with on-chip PPy is robust and sensitive. The  
7  
8 electrodeposition of PPy was carried out both on precious (platinum, gold, and palladium) and non-  
9  
10 precious metal electrodes (iron and nickel), demonstrating that the polymerization can be  
11  
12 performed with metals that are currently used in a standard semiconductor foundry. Also, the PPy  
13  
14 quasi-reference electrodes were fabricated on foundry ISFET chips and used to bias the transistor  
15  
16 fluid-gate during pH sensing experiments. The sensing performance of ISFETs biased with on-chip  
17  
18 PPy is similar to that obtained when the transistor is biased with Ag/AgCl. The similar results  
19  
20 obtained with these two kinds of electrodes indicate that the high stability and low pH response of  
21  
22 the PPy quasi-reference translates to the ISFET system, allowing robust operation of the transistor  
23  
24 as pH sensor with a microreference.  
25  
26  
27  
28  
29  
30  
31  
32  
33  
34  
35  
36  
37  
38  
39  
40  
41  
42  
43  
44  
45  
46  
47  
48  
49  
50  
51  
52  
53  
54  
55  
56  
57  
58  
59  
60

## 2. Experimental section

### 2.1 Patterning on-chip microelectrodes:

Metal microelectrodes are patterned on oxidized silicon wafers and ISFET chips with a standard lift-off process. Positive photoresist SPR 220-4.5 (Microchem, Westborough, MA) is spin coated and UV-patterned on the substrate. Metals are then deposited using an E-beam evaporator (CHA Industries, Fremont, CA) having a 250 Å titanium adhesion layer and 350 Å of the metal selected to form the electrode. After metal evaporation the wafer is immersed in Remover PG (Microchem), sonicated for 15 min, and rinsed with isopropanol and DI water.

### 2.2 Electrochemical polymerization of polypyrrole on microelectrodes:

Partially oxidized PPy has been deposited in the past on platinum and stainless steel wires through a cyclic voltammetry deposition process for the formation of quasi-reference electrodes.<sup>23</sup> This technique is frequently used to form electrodes for scanning electrochemical microscopy assays.<sup>26</sup> We used a similar method to deposit the PPy on patterned metal leads to form on-chip electrodes to bias the electrolyte. Figure 1(a) shows a schematic of the three-electrode cell for PPy polymerization and deposition in patterned metal microelectrodes. A polydimethylsiloxane (PDMS) well is bonded to the silicon substrate, the on-chip metal is electrically contacted with a micromanipulator probe, a graphite rod is inserted in the solution, and a Ag/AgCl reference electrode (BASi, West Lafayette, IN) is bridged with a pipette tip filled with Agar gel and 0.1 M NaClO<sub>4</sub> for minimization of a liquid junction potential between the organic solvent and the aqueous filling solution in the reference electrode. The well is then filled with 400 μL of acetonitrile containing 10 mM pyrrole and 100 mM of Tetrabutylammonium hexafluorophosphate (all chemicals from Sigma-Aldrich). Figure S1 presents a photograph of the electrochemical cell used in the PPy polymerization on the microelectrode.

The three electrodes are connected to a Reference 600™ potentiostat (Gamry Instruments, Warminster, PA) that performs cyclic voltammetry (CV), sweeping the potential from -0.6 to 1.2 V at a 100 mV/s rate and an initial/final potential of 0.4 V. The CV process is repeated for the desired number of cycles, depositing the polymer on the working electrode. In every iteration, pyrrole is polymerized and a dark film of partially oxidized polypyrrole (PPy/PPy<sup>+</sup>PF<sub>6</sub><sup>-</sup>) is formed on the exposed microelectrode.

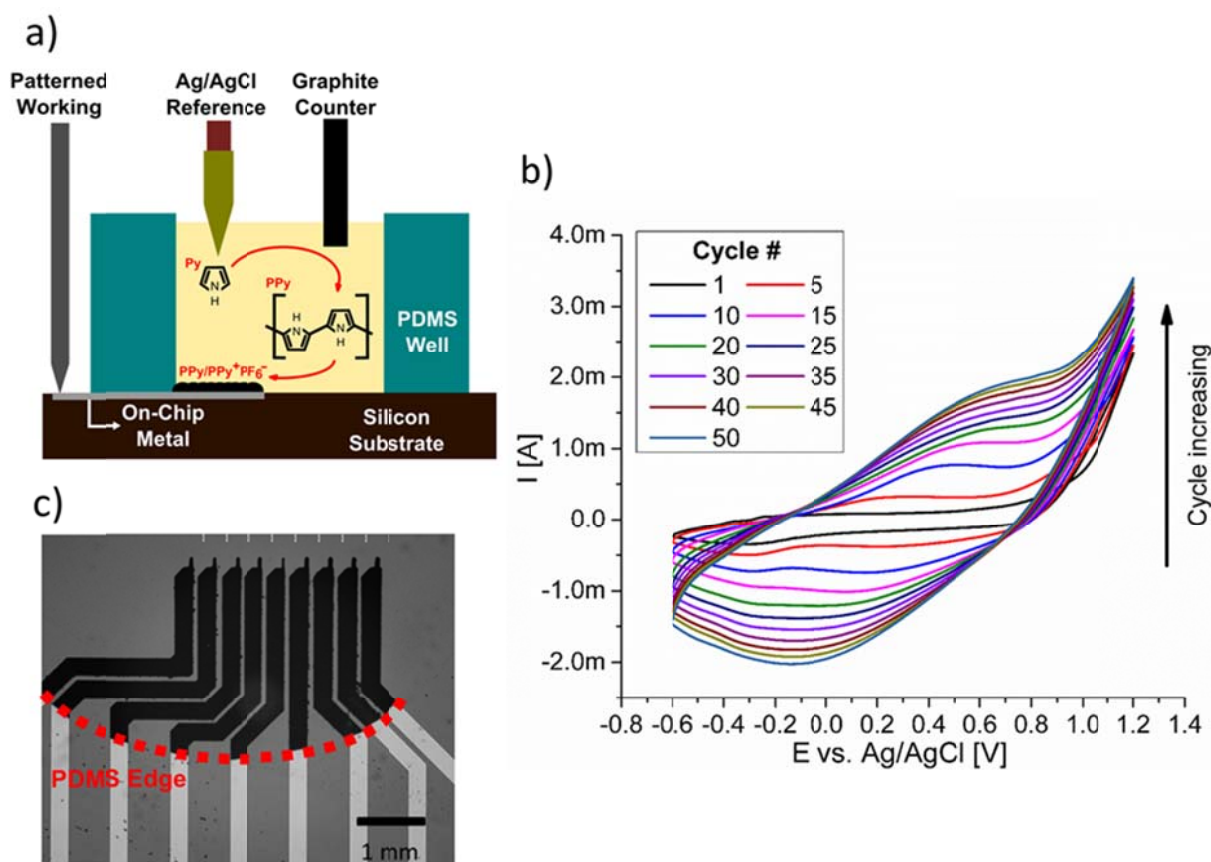


**Fig. 1** Electrodeposition of PPy on on-chip patterned metal electrodes. **(a)** Schematic of the three-electrode cell used for deposition and schematic of the polymerization. The PDMS well is filled with the acetonitrile solution with pyrrole that gets polymerized during CV leaving a film of partially oxidized PPy on the microelectrode. **(b)** Typical deposition of PPy on platinum microelectrodes by CV, the peak currents increase in each cycle as the PPy electrode grows. **(c)** Image of independent on-chip platinum electrodes coated with the PPy layer. The edge of the PDMS well is clearly defined owing to the fact that only on-chip metal exposed to the acetonitrile solution is coated.

### 2.3 Physical characterization of film:

The polypyrrole film deposited in electrodes was characterized using profilometer and goniometer measurements, optical and SEM imaging, and X-Ray diffraction (XRD) analysis. The reported membrane thickness is the total indicator runout (TIR) obtained in a step-high profilometer measurement and the total height of the roughness profile (Rt parameter) is retrieved after applying a 2CR filter to the acquired data. To assess hydrophilicity of the membranes, contact angle measurements were performed on larger electrodes to accommodate 3  $\mu$ L water droplets. In addition, bright field and SEM images of electrodes were taken with different numbers of PPy coating cycles to evaluate the growth of PPy. The area of the PPy electrode is quantified with ImageJ using the number of dark pixels in the bright field images. Finally, to assess the structural composition of the deposited PPy film, XRD patterns of the electrodeposited polymer were obtained in a continuous scan from 5 ° to 105 ° in a PANalytical/ Philips X'pert MRD system.

### 2.4 Open circuit potential measurements:

Open circuit potential (OCP) measurements were taken to evaluate stability and response to pH changes of the fabricated microelectrodes. For stability experiments, the PDMS reservoir was filled with a 10 mM KCl solution, the Ag/AgCl (unbridged) electrode was used as the reference, and the on-chip metal was set as the working electrode. The potentiostat was programmed to take OCP measurements every half second for one hour after the initial 600 s of stabilization, and each experiment was repeated 3 times. For the pH response analysis, the KCl solution in the PDMS reservoir was spiked with 10 mM HCl or NaOH during the OCP measurement and the pH value was calibrated with an InLab® ultra-micro pH electrode (Mettler-Toledo, Columbus, OH). After the injection, the potential is allowed to stabilize for 600 s and the last 50 s of measurements are averaged to obtain the OCP value for each pH. A pH range of 5.5-8.5 was selected for sensitivity

1  
2  
3  
4  
5  
6 characterization experiments in order to model the behavior of electrodes in regular physiological  
7 buffers and a typical reaction mix of biomolecular assays such as DNA amplification.<sup>22</sup>  
8

9  
10 The OCP measurements without pH changes are used to quantify stability, repeatability, and drift of  
11 the electrodes under evaluation. Stability is the potential variation during a one hour experiment,  
12 and is determined by taking the standard deviation of all measurements in an experiment.  
13 Repeatability is the variation across the different experiments and is calculated using the average of  
14 the standard deviations of measurements in three experiments. The drift measures the changes in  
15 potential as a function of time and is the difference of the recorded potentials at the beginning and  
16 the end of the experiment. Lastly, the reported pH sensitivity is the absolute value of the slope in a  
17 linear regression of the OCP vs. pH data.  
18  
19  
20  
21  
22  
23  
24  
25  
26  
27  
28  
29

### 30 2.5 ISFET Fabrication:

31  
32 ISFET devices were fabricated by Taiwan Semiconductor Manufacturing Company (Hsinchu,  
33 Taiwan) with a standard semiconductor process performed on silicon-on-insulator wafers. A  
34 complementary metal-oxide-semiconductor (CMOS) process forms the transistor in the device  
35 silicon layer. This process is followed by a metallization layer that defines contacts to drain/source  
36 nodes and a metallic extended gate that will act as the sensing region. Then, the top inter-layer  
37 dielectric is deposited and selectively dry-etched to create openings that reveal the metallic  
38 extended gate. The ISFETs are finalized with the deposition of atomic layer deposition (ALD)  
39 hafnium oxide over the entire wafer, creating the oxide sensing membrane on top of the extended  
40 gate. The use of hafnium oxide as the sensing layer on ISFET pH sensors has been reported in the  
41 past. Our group demonstrated that ISFETs made with HfO<sub>2</sub> had a sensitivity of 56mV/pH, with high  
42 linearity, over a range between pH 4-10.<sup>27</sup> Other publications have also reported the use of HfO<sub>2</sub> as  
43 the sensing layer in ISFETs for larger ranges (pH 2-12),<sup>28</sup> and extended-gate transistors that use  
44  
45  
46  
47  
48  
49  
50  
51  
52  
53  
54  
55  
56  
57  
58  
59  
60

1  
2  
3  
4  
5  
6 high-K dielectrics report high sensitivity and linearity.<sup>29</sup> In Fig. S2 we present pH dependent  
7 transistor transfer curves of ISFETs to characterize performance of HfO<sub>2</sub> ISFETs used in this study.  
8  
9

## 10 11 12 13 14 15 2.6 ISFET testing:

16  
17 To operate ISFETs, source, drain, and gate nodes of the transistors are connected to independent  
18 source measure units (SMUs) of a Keithley 4200scs (Keithley, Columbus, OH), and a PDMS well is  
19 plasma-bonded to the chip to hold the electrolyte solutions. The transistor fluid gate is swept from -  
20 1 to 1 V to obtain transfer characteristic curves that are used to extract threshold voltages using a  
21 constant-current extraction method having  $I_{th} = 300 \text{ nA} * \frac{W}{L}$ , where  $\frac{W}{L}$  is the transistor's aspect  
22 ratio.<sup>30</sup> In stability tests, the threshold voltage is measured every minute for an hour to quantify  
23 stability and drift. For pH sensitivity experiments, the electrolyte in the PDMS reservoir is titrated  
24 with 10 mM NaOH or HCl, and the resulting changes in the threshold voltage are correlated with  
25 surface potential to obtain the ISFET pH sensitivity. Testing buffers were selected in the range of  
26 pH 6-8 to model the sensor performance in physiological buffers, the master mix of molecular  
27 reactions such as PCR or LAMP, or solutions used in protein binding assays.<sup>5</sup>  
28  
29  
30  
31  
32  
33  
34  
35  
36  
37  
38  
39  
40  
41

## 42 3. Results and Discussion

### 43 44 3.1 Deposition of polypyrrole on microelectrodes:

45  
46 The electrodeposition of PPy in the patterned microelectrodes was carried out in the three-  
47 electrode electrochemical cell that is illustrated in Fig. 1(a). Cyclic voltammetry between working  
48 and counter electrodes referenced to a bridged Ag/AgCl creates a dark film of partially oxidized PPy  
49 in the electrodes that are exposed to the electrolyte. Voltammograms from a typical CV deposition  
50 process are presented in Fig. 1(b), which shows the expected shape of CV curves and greater  
51 peak/valley currents as the PPy film grows.<sup>23,31</sup> Figure 1(c) shows PPy-coated platinum  
52  
53  
54  
55  
56  
57  
58  
59  
60

1  
2  
3  
4  
5  
6  
7  
8  
9  
10  
11  
12  
13  
14  
15  
16  
17  
18  
19  
20  
21  
22  
23  
24  
25  
26  
27  
28  
29  
30  
31  
32  
33  
34  
35  
36  
37  
38  
39  
40  
41  
42  
43  
44  
45  
46  
47  
48  
49  
50  
51  
52  
53  
54  
55  
56  
57  
58  
59  
60

microelectrodes on an oxidized wafer. Each electrode was set as the working electrode in independent polymerizations, showing that the process is repeatable and will cover the full electrode that is exposed to the acetonitrile solution.

Figure 2 presents results of PPy film characterization analysis. Profilometer measurements were carried out on electrodes with different deposition cycles to examine the evolution of the PPy film thickness and roughness. Figure 2(a) shows that the film quickly grows to a few microns in the initial cycles and proceeds to grow linearly in subsequent iterations, reaching around 25  $\mu\text{m}$  at the end of the 50<sup>th</sup> cycle. A similar trend is observed in the roughness of the growing film. Figure 2(b) shows that a thicker layer is correlated with a rougher electrode, indicating uneven growth of the PPy layer. In addition, Fig. 2(d) shows that more cycles result in more hydrophilic electrodes. The well-known enhancement relationship between roughness and wettability<sup>32</sup> explains the observed trend of lower contact angles as the hydrophilic PPy layer becomes rougher. The high wettability of the PPy electrodes will simplify their use for applications that use small volumes or droplets. Contact between an on-chip electrode and small volumes can be cumbersome with other approaches that use hydrophobic membranes and therefore would require mechanisms for volume confinement.<sup>33</sup>

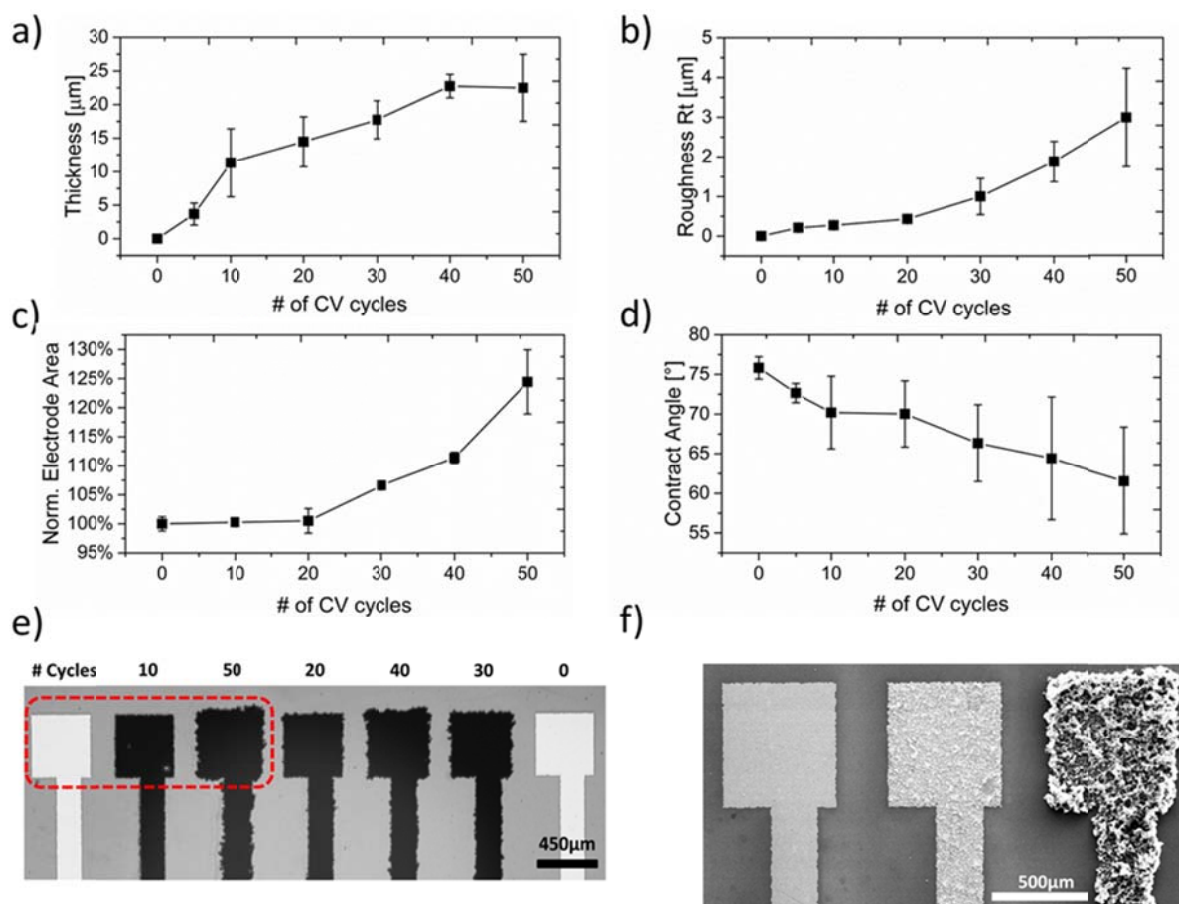


**Fig. 2** Characterization of the deposited PPy film. **(a)** Film thickness, **(b)** Profilometry total roughness (Rt), **(c)** Normalized area of the electrode, and **(d)** contact angle, as a function of the CV deposition cycles. **(e)** Optical image of square electrode array with different numbers of deposition cycles. **(f)** Scanning electron microscopy image of electrodes in the left side of the array presenting 0, 10, and 50 deposition cycles.

Figures 2(e) and 2(f) are bright field and SEM images of electrodes with different CV deposition cycles. They reveal the uneven and isotropic growth of the polymer layer. The bright field images show that electrodes with more PPy have a larger area and an irregular shape. Figure 2(c) presents the quantified relative growth of the electrode area as a function of the number of polymerization cycles. It shows that during the initial cycles the measured area is the same as that of the original electrode indicating that the PPy film grows mostly perpendicular to the silicon. However, in later cycles the PPy layers grow stacked on top of each other resulting in the observed isotropic growth. Figure 2(f) zooms in on the left portion of the electrode array (for 0, 10, and 50 cycles) and clearly

1  
2  
3  
4  
5  
6 shows that the PPy film becomes thicker and rougher as it grows. The isotropic growth and  
7  
8  
9  
10  
11  
12  
13  
14  
15  
16  
17  
18  
19  
20  
21  
22  
23  
24  
25  
26  
27  
28  
29  
30  
31  
32  
33  
34  
35  
36  
37  
38  
39  
40  
41  
42  
43  
44  
45  
46  
47  
48  
49  
50  
51  
52  
53  
54  
55  
56  
57  
58  
59  
60  
shows that the PPy film becomes thicker and rougher as it grows. The isotropic growth and  
variability of the deposition process will limit the spatial resolution of the PPy electrodes. The  
horizontal growth of the polymer (parallel to the chip) may cause undesired shorts between  
patterned electrodes and PPy coating of regions adjacent to electrodes. Therefore, the design of  
photolithography masks for the lift-off process must take into account this lateral growth and  
provide adequate spacing between electrodes and on-chip features to prevent shorts or undesired  
PPy coating during the polymerization. In addition, Fig. S3 shows X-ray diffraction patterns for PPy  
films deposited on platinum and nickel patterned electrodes. In both cases we observed expected  
peaks from metal and substrate in addition to peaks at around  $24^\circ$ . These peaks arise from the  $\pi$ -  
bonds interaction of the PPy chains and it is correspond to a  $d$  spacing of 0.38.<sup>34</sup> These results  
indicate that the on-chip electrodeposition yield a normal PPy film that can be used in the  
electrochemical operations.

### 3.2 Stability of polypyrrole microelectrodes:

The stability of on-chip microelectrodes fabricated with different metals, with and without the PPy  
film, was quantified with open circuit potential (OCP) measurements against a standard Ag/AgCl  
reference electrode. For each experiment, OCP measurements were collected for one hour because  
biochemical reactions that are monitored with ISFETs, such as DNA amplification<sup>35</sup> or protein  
binding,<sup>36</sup> normally occur within that time frame. Figure 3(a) shows the measured OCP as a  
function of time for platinum and gold electrodes with and without PPy. The same figure also shows  
an OCP stability measurement between two Ag/AgCl electrodes that is used as a benchmark. Data  
in Fig. 3(a) is presented in the form of “bands” where the thickness is correlated to repeatability of  
OCP measurements. Each time point for each curve in this plot represents 3 averaged experiments  
at the same time point with the calculated standard deviation plotted as the error bar. The error  
bars, which are in close proximity because measurements were taken every half second, create the

1  
2  
3  
4  
5  
6 effect of a thick band. Therefore, the thickness of each band is a representation of the electrode  
7 repeatability, and variations in the profile represent the electrode stability. Comparative  
8 quantifications of stability and drift are in Fig. 3(b) and 3(c). The PPy coating makes the electrodes  
9 more stable, reducing the variability by around one order of magnitude, and substantially reduce  
10 drift. The best results were obtained with PPy coated platinum that has stability and drift  
11 comparable to the commercial Ag/AgCl electrode. Although the commercial reference electrode is  
12 better than those fabricated with polypyrrole, their stability and possibilities for miniaturization  
13 make the PPy electrodes an interesting alternative to the conventional reference electrodes for  
14 ISFET operation.  
15  
16  
17  
18  
19  
20  
21  
22  
23  
24  
25  
26  
27  
28  
29  
30  
31  
32  
33  
34  
35  
36  
37  
38  
39  
40  
41  
42  
43  
44  
45  
46  
47  
48  
49  
50  
51  
52  
53  
54  
55  
56  
57  
58  
59  
60

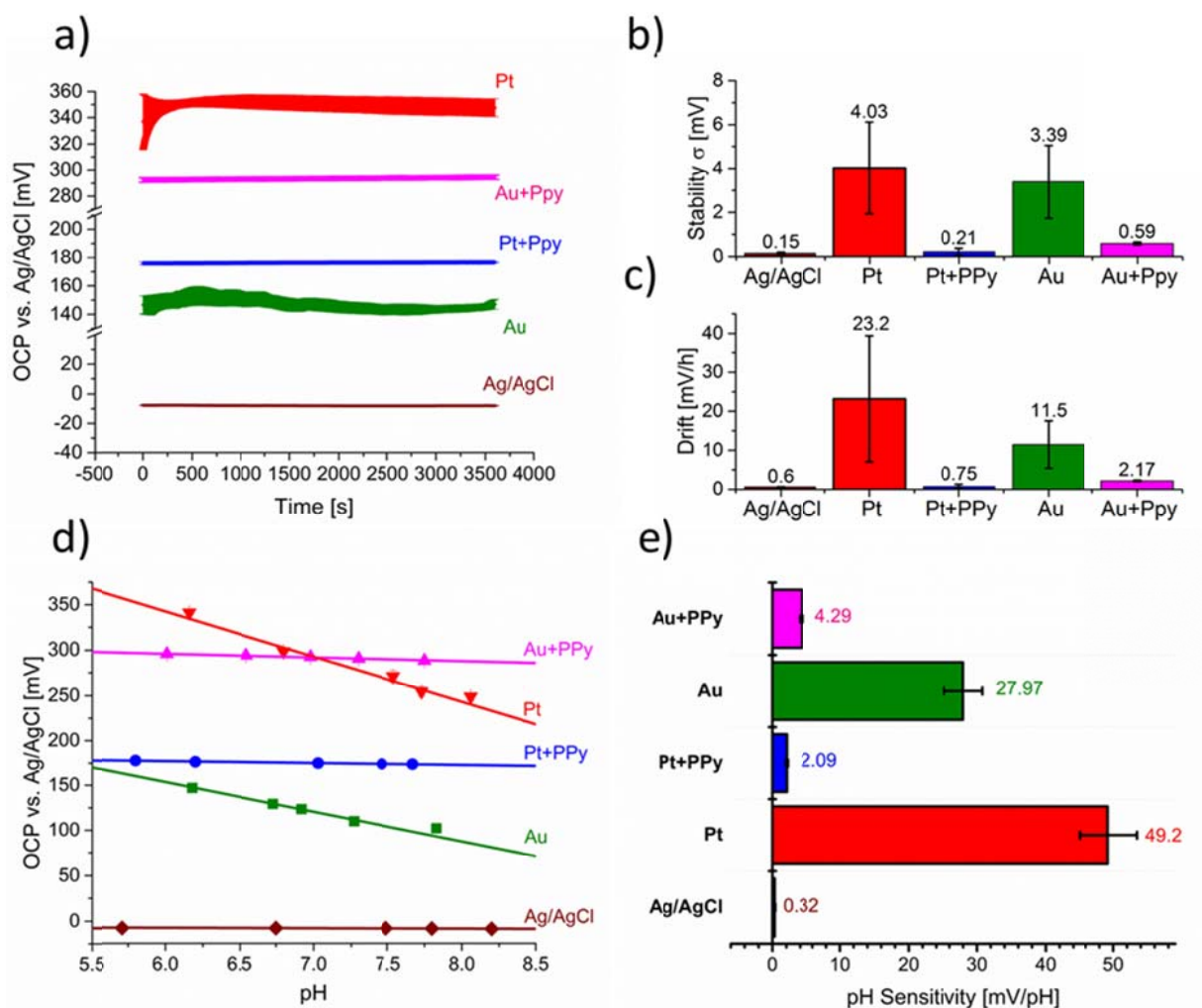


**Fig. 3** Open circuit potential (OCP) measurements of electrode stability and pH sensitivity in a 10mM KCl solution. **(a)** OCP vs. Ag/AgCl as a function of time for each electrode. The bands represent 3 experiments, having the thickness is correlated with repeatability, and fluctuations reflecting stability and drift.

Comparative quantification of **(b)** stability and **(c)** drift of OCP measurements showing improved performance with PPy. **(d)** Measured OCP as a function of the electrolyte pH with the calculated linear regressions. **(e)** Extracted pH sensitivity for each electrode demonstrating reduced pH response of the PPy electrodes.

### 3.3 pH sensitivity of electrodes:

Besides providing a stable potential during the experiment, a reference electrode needs to sustain a constant voltage despite changes in the electrolyte.<sup>14</sup> Figure 3(d) presents the pH sensitivity of gold, platinum, and Ag/AgCl electrodes measured by monitoring the OCP as a function of the electrolyte's pH. Individual plots for each experiment with a different scale that show details of the pH response

1  
2  
3  
4  
5  
6 for each electrode are in the supplementary Figure S4. The ideal reference electrode response to  
7 pH changes is the one observed for the Ag/AgCl reference electrode. With this electrode, despite  
8 electrolyte pH variations, the OCP potentials are within 1 mV, resulting in a very low pH sensitivity.  
9  
10 This is a consequence of the Nernst equation for the Ag/AgCl electrode that is independent of H<sup>+</sup>  
11 ions. Experiments with other electrodes show potential variations as a function of pH. The  
12 deprotonation and protonation of the electrode's surface is a function of the solution's pH and  
13 affects the electrode-localized potential, resulting in pH-dependent OCP.<sup>37</sup> Other publications have  
14 reported similar trends and quantification of the sensitivity of metal electrodes to pH changes.<sup>38</sup>  
15 However, electrodes coated with the PPy film are substantially less sensitive to pH changes than  
16 their bare metal counter parts. The partially oxidized PPy film deposited on the on-chip electrodes  
17 is posed by the half reaction  $PPy^+A^- + e \rightleftharpoons PPy + A^-$  that allows exchange of ions to sustain a  
18 stable potential.<sup>23</sup> The pH titration experiments are summarized in Fig. 3(e), which compares pH  
19 sensitivity of different electrodes. Potentials measured with platinum electrodes are known to have  
20 high pH dependence,<sup>22</sup> but after the PPy polymerization the pH sensitivity is reduced by more than  
21 10 times. A similar pH sensitivity reduction is observed for the gold electrode. The PPy layer brings  
22 new ion dynamics that result in low pH sensitivities that are significantly smaller than in bare metal  
23 electrodes and are required to reference an ISFET.  
24  
25  
26  
27  
28  
29  
30  
31  
32  
33  
34  
35  
36  
37  
38  
39  
40  
41  
42  
43  
44

#### 45 3.4 Non-precious metals electrodes:

46  
47 Lack of compatibility with semiconductor processes and high manufacturing costs explain why  
48 previously reported strategies to create on-chip reference electrodes have not been fully adopted  
49 for ISFET operation.<sup>39</sup> The PPy deposition process has been widely reported in gold and platinum  
50 wires, but to reduce cost and enable simpler implementation it is necessary to perform the  
51 electrodeposition process in non-precious metals. The CV deposition process has been also carried  
52 out on a stainless steel wire<sup>23</sup> and others have reported deposition on aluminum at the expense of  
53  
54  
55  
56  
57  
58  
59  
60

1  
2  
3  
4  
5  
6  
7  
8  
9  
10  
11  
12  
13  
14  
15  
16  
17  
18  
19  
20  
21  
22  
23  
24  
25  
26  
27  
28  
29  
30  
31  
32  
33  
34  
35  
36  
37  
38  
39  
40  
41  
42  
43  
44  
45  
46  
47  
48  
49  
50  
51  
52  
53  
54  
55  
56  
57  
58  
59  
60

modifying the electrolyte solution, adding polishing steps, and using electron transfer mediation techniques.<sup>40</sup> To facilitate adaptation of the PPy reference microelectrodes to other standardized fabrication techniques, we attempted the same simple CV PPy deposition process, used in gold and platinum, in metals compatible with CMOS microfabrication steps and evaluated their performance. The PPy polymerization was also performed on palladium on-chip microelectrodes. Although it is an expensive precious metal, palladium has been used to improve reliability and thermal stability of contact electrodes in MOSFETs and can be incorporated in the CMOS semiconductor processes.<sup>41</sup> Results are presented in Figure S5, which shows normal cyclic voltammograms during the deposition process, stable OCP measurements, and a substantial reduction in the pH sensitivity. The next polymerization experiment was performed in iron microelectrodes. The previous polymerization of the PPy layer in steel suggested that iron, which is not currently used for CMOS processes but is an inexpensive commodity material, could be used as a microelectrode in the deposition process. Figure S6 shows that despite irregular cyclic voltammograms and unexpected reduction of peak currents during the CV process, the deposition of PPy drastically improves stability and pH sensitivity of the electrode. This shows that the PPy coated iron is a stable quasi-reference electrode with performance equivalent to that of the PPy electrodes that use precious metals.

The CV polymerization experiments were also performed with metals that are commonly used in semiconductor foundries. Electrodeposition of PPy on metals that are currently used for metallization layers in the CMOS manufacturing process would strongly facilitate the incorporation of these electrodes in the fabrication process to create on-chip quasi-reference electrodes. In this case, reference electrodes could be easily created in a new metal layer in the surface of the chip that would be coated with PPy using the CV electrodeposition, with no need of additional masks or lithography steps simplifying fabrication. With the same deposition protocol described above we were able to deposit the PPy film on nickel microelectrodes but not on copper, titanium, or

aluminum. Although nickel is not used for metal leads in the CMOS process, it is commonly used to create low-resistance nickel-silicide contacts that interface silicon and metal layers in the source and drain nodes.<sup>42</sup> Figure 4(a) presents the deposition CVs on nickel, showing the expected trend of greater peak currents as the layer grows. These curves also show a secondary process around -0.2 V in reduction. Nevertheless, that process is eliminated in the later cycles, and the final voltammograms are similar to those observed in the deposition on precious metals. Figure 4(b) presents the stability measurements and Fig. 4(c) shows the pH sensitivity results for both bare nickel and nickel coated with the PPy layer. Once again, quantification of the stability and pH sensitivity demonstrate that the PPy layer significantly reduces potential variations and the response to pH changes of the nickel electrode, demonstrating that it is possible to create an on-chip quasi-reference electrode with a metal used in a semiconductor foundry.

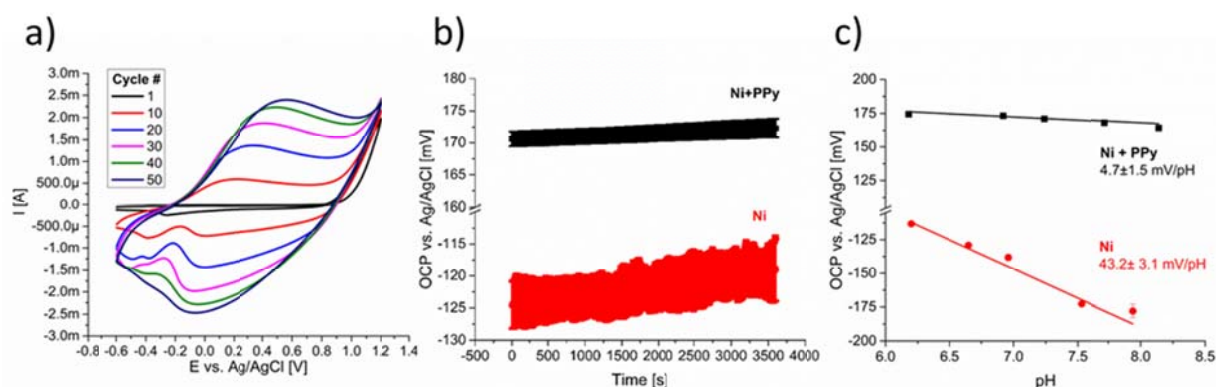


**Fig. 4** Polymerization of PPy on nickel electrodes and electrical performance evaluation. **(a)** CV deposition of PPy film on nickel microelectrodes. **(b)** Bands of OCP stability as a function of time for nickel with and without the PPy layer. **(c)** OCP vs. electrolyte pH to assess pH sensitivity of nickel and nickel+PPy electrodes.

The results of the linear regressions are reported as sensitivity.

The electrodeposition of PPy in the other metals typically used in semiconductor foundries suffered from low metal reduction potentials that resulted in the dissolution of the metal thin-film during the CV process, or high resistivity of metals and metal oxides that prevented PPy film formation.

1  
2  
3  
4  
5  
6 Previous publications have described other approaches to deposit PPy on these metals.<sup>40,43,44</sup>  
7  
8 Nevertheless, those approaches were not pursued because they include additional steps that would  
9  
10 complicate the deposition process, undermining desired CMOS compatibility and protocol  
11  
12 simplicity. The results of the attempted electrodepositions on copper, aluminum and titanium,  
13  
14 including further discussion are presented in the supplementary information (Figures S7-S9).

15  
16  
17 Table 1 summarizes the stability and pH sensitivity data for all the electrodes where PPy  
18  
19 polymerization was successful, including data for their bare metal counter parts. For all metals, the  
20  
21 metal/PPy electrodes presented better stability, improved repeatability, lower drift, and reduced  
22  
23 pH response. It is important to note that pH sensing with bare metal electrodes was in general  
24  
25 unreliable and only linear in small pH ranges. However, the pH sensitivity evaluation through linear  
26  
27 regressions of OCP vs. pH data created a standard metric that enabled comparisons between  
28  
29 electrodes and demonstrated a clear reduction of the pH sensitivity with PPy electrodes. The main  
30  
31 conclusion to be drawn from table 1 and from the different OCP experiments is that patterned  
32  
33 microelectrodes coated with PPy are more stable and less sensitive to pH changes than the metal-  
34  
35 only electrodes. Therefore, PPy electrodes are better candidates for on-chip quasi-reference  
36  
37 electrodes to operate ISFETs.  
38  
39  
40  
41  
42  
43  
44  
45  
46  
47  
48  
49  
50  
51  
52  
53  
54  
55  
56  
57  
58  
59  
60

Electrode	Stability [mV]	Repeatability [mV]	Drift [mV/h]	pH sensitivity [mV/pH]
Platinum	4.03 ± 2.09	6.10 ± 1.82	23.2 ± 16.2	49.2 ± 4.25
Platinum + PPy	0.21 ± 0.16	0.67 ± 0.17	0.75 ± 0.53	2.09 ± 0.16
Gold	3.38 ± 1.66	4.42 ± 1.19	11.5 ± 6.07	27.97 ± 2.81
Gold + PPy	0.59 ± 0.06	1.63 ± 0.05	2.17 ± 0.18	4.29 ± 0.28
Palladium	3.32 ± 0.42	10.7 ± 0.42	10.6 ± 0.52	36.2 ± 3.5
Palladium + PPy	0.21 ± 0.12	0.48 ± 0.13	0.92 ± 0.43	8.61 ± 0.57
Nickel	1.72 ± 0.35	3.64 ± 0.4	7.12 ± 1.5	43.19 ± 3.12
Nickel + PPy	0.51 ± 0.10	1.28 ± 0.08	1.73 ± 0.36	4.7 ± 1.56
Iron	6.91 ± 1.11	5.37 ± 2.8	35.8 ± 7.25	29.5 ± 2.03
Iron + PPy	0.44 ± 0.06	1.87 ± 0.05	1.57 ± 0.26	4.71 ± 1.23

**Tab. 1** Summary of stability, repeatability, drift, and pH sensitivity of electrodes made with different metals and with/without the deposited PPy film.

### 3.5 Operation of ISFET with PPy electrodes:

Platinum microelectrodes were patterned on an ISFET chip with the lift-off process described previously. The same electrochemical cell used for other PPy depositions on electrodes (Fig. 1(a)) was used for the ISFET chip. A PDMS well is bonded to the top of the silicon die and is filled with the acetonitrile solution. Then, the graphite counter and the bridged Ag/AgCl electrodes are placed inside the well. The deposition cyclic voltammograms are similar to the others reported previously but have lower current peaks because the electrodes on the ISFET chip have a smaller area than the testing structures (Fig. S10). On the same chip, platinum leads were coated with PPy but others were left exposed for comparative measurements. The result is presented in Fig. 5(a), which shows

an extended gate ISFET surrounded by a PPy electrode and an exposed platinum electrode in close proximity.

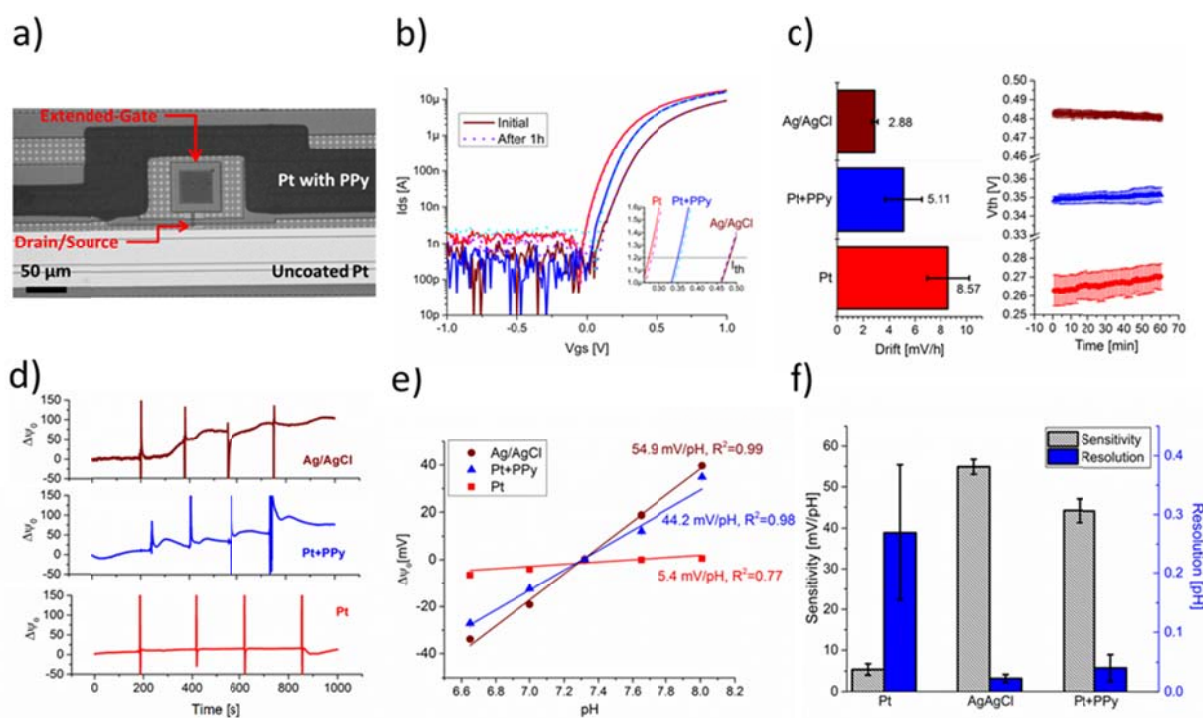


**Fig. 5** Evaluation of ISFET operation with PPy microelectrodes. **(a)** Image of an extended-gate ISFET surrounded by a platinum+PPy and bare platinum electrodes used for comparative measurements. **(b)** ISFET transfer characteristics with platinum, PPy, and Ag/AgCl fluid-biasing electrodes. Solid lines represent the first measurement and dotted lines the last measurement in a one hour experiment. The inset zooms in the area for constant current threshold voltage calculation. **(c)** Quantification of threshold voltage drift with each electrode and plot of threshold voltage as a function of time during a one hour experiment. Error bars represent variation between different experiments **(d)** Real time surface potential variations due to pH changes. The spikes every 200s in the plot indicate injection of NaOH in the PDMS reservoir and the electrolyte pH-values are the same ones that is plotted in literal 'e'. **(e)** ISFET surface potential as a function of pH with linear regressions to quantify sensitivity. **(f)** Comparative results of pH sensitivity and resolution of the ISFET operation with each electrode.

After the polymerization process, the acetonitrile solution is switched to a 10mM KCl solution for stability and pH experiments. To modulate drain current, the transistor's fluid-gate is biased with the on-chip electrodes (platinum and PPy) and also with a commercial Ag/AgCl reference electrode. Transfer characteristics of the transistor are presented in Fig. 5(b), where the inset zooms in the region where the threshold voltage is determined. Operation with the 3 electrodes yielded standard

1  
2  
3  
4  
5  
6 transfer characteristics similar to those from other devices with the same fabrication process. The  
7  
8 stability of the transistor is evaluated by measuring transfer characteristics every minute for an  
9  
10 hour with each electrode in 3 separate experiments. The extracted threshold voltage as a function  
11  
12 of time is plotted in Fig. 5(c), along with bars that quantify the threshold voltage drift. As expected,  
13  
14 the best stability results are obtained with the commercial Ag/AgCl electrode, the worst with the  
15  
16 bare platinum electrode, and intermediate results with the PPy electrode. It is clear that the  
17  
18 potential applied to the transistor is more stable and repeatable when the patterned platinum is  
19  
20 coated with PPy. Also, the voltage variations and drift are greater in the ISFET experiment than in  
21  
22 OCP measurements. This indicates that new noise sources related to the ISFET operation, such as  
23  
24 thermal voltage fluctuations or stochastic electrochemical interactions in the gate oxide,<sup>45</sup> harm the  
25  
26 transistor's voltage stability.  
27  
28

29  
30 Evaluation of the ISFET pH sensitivity was performed by measuring threshold voltage variations  
31  
32 due to pH changes and correlating them with the change in the oxide surface potential. The same  
33  
34 evaluation was performed by biasing the electrolyte with the platinum, PPy, and Ag/AgCl  
35  
36 electrodes to compare ISFET pH sensing performance. Figure 5(d) shows the extracted surface  
37  
38 potential as a function of time while the electrolyte pH is changed by titrating NaOH and the full pH-  
39  
40 dependent transfer curves are presented in Fig. S11. Even though there is a clear pH response with  
41  
42 the Ag/AgCl and PPy electrodes, the high pH sensitivity of the platinum electrode counteracts the  
43  
44 ISFET response, thereby diminishing the recorded surface potential changes in the ISFET. This  
45  
46 same behavior has been reported previously and constitutes a strong argument against using  
47  
48 platinum electrodes as quasi-reference electrodes for pH monitoring with ISFETs.<sup>22</sup> The  
49  
50 quantification of the pH sensitivity is presented in Fig 5(e), which plots normalized changes in  
51  
52 surface potential as a function of the electrolyte pH for the three electrodes. The linear regressions  
53  
54 quantify sensitivity and show that the ISFET has sensitivity close to the Nernstian limit when  
55  
56 operated with Ag/AgCl, a lower but similar response with the PPy electrode, and very low  
57  
58  
59  
60

1  
2  
3  
4  
5  
6 sensitivity with the platinum electrode. This quantification underscores the importance of  
7  
8 minimum pH response of the quasi-reference electrodes. Good ISFET operation is achieved when  
9  
10 only the transistor's surface potential changes as a function of the electrolyte pH. Otherwise, other  
11  
12 secondary interactions between potentials can undercut pH sensitivity and the ISFET performance.  
13  
14 Figure 5(f) compares the pH sensitivity and resolution of ISFETs biased with the different  
15  
16 electrodes. The pH resolution is defined as the ratio of noise to sensitivity ( $\Delta pH_{min} = \sigma\psi_s/S$ ),  
17  
18 where  $\sigma\psi_s$  is the average of potential fluctuations in each pH measurement (noise), and  $S$  is the  
19  
20 extracted sensitivity.<sup>35</sup> From this plot we conclude that ISFET pH sensitivity can be greatly  
21  
22 improved by coating the microelectrode with the PPy layer. The greater stability and lower  
23  
24 dependence of the PPy/electrolyte potential to pH changes result in the ability to sense smaller pH  
25  
26 fluctuations (of around 0.04 pH units), which would translate into faster response times and lower  
27  
28 detection limits in the biochemical assays. Therefore, the addition of the PPy layer turns patterned  
29  
30 microelectrodes into a robust reference for ISFET operation.  
31  
32  
33

34 A similar pH sensing evaluation was performed for ISFETs operated with nickel-based electrodes.  
35  
36 Cyclic voltammograms of the PPy deposition on nickel microelectrodes are presented in Fig. S10  
37  
38 that shows expected shapes but low current. Figure 6 presents measured sensitivity and stability of  
39  
40 an ISFET biased with a Ni+PPy electrode and compares it with results obtained using a bare Ni  
41  
42 electrode. Figure 6(a) shows pH-dependent transfer curves when the ISFET is operated with a  
43  
44 Ni+PPy electrode. As shown in Fig. 6(b), the sensitivity quantification yielded a surface potential  
45  
46 change of  $\sim 39$  mV/pH. This is significantly larger than the 15 mV/pH obtained with a bare Ni  
47  
48 electrode. In addition, the Ni+PPy electrodes are more stable than the bare Ni counterpart. Figure  
49  
50 6(c) shows the ISFET threshold voltage as a function of time during one hour, demonstrating that  
51  
52 measurements performed with Ni+PPy electrodes are more repeatable and have lower noise levels.  
53  
54 Comparative measurements of pH resolution and total drift are presented in Fig. 6(d) that  
55  
56 summarizes the characteristics of Ni+PPy electrodes. The fine pH resolution and low threshold  
57  
58  
59  
60

voltage drift of the ISFET biased with Ni+PPy is consistent with the low pH dependence and high stability observed for coated nickel electrodes in OCP measurements. With both Ni and Pt the electrodeposition of PPy on the patterned electrodes created a robust reference that translates into higher sensitivities and lower noise levels.

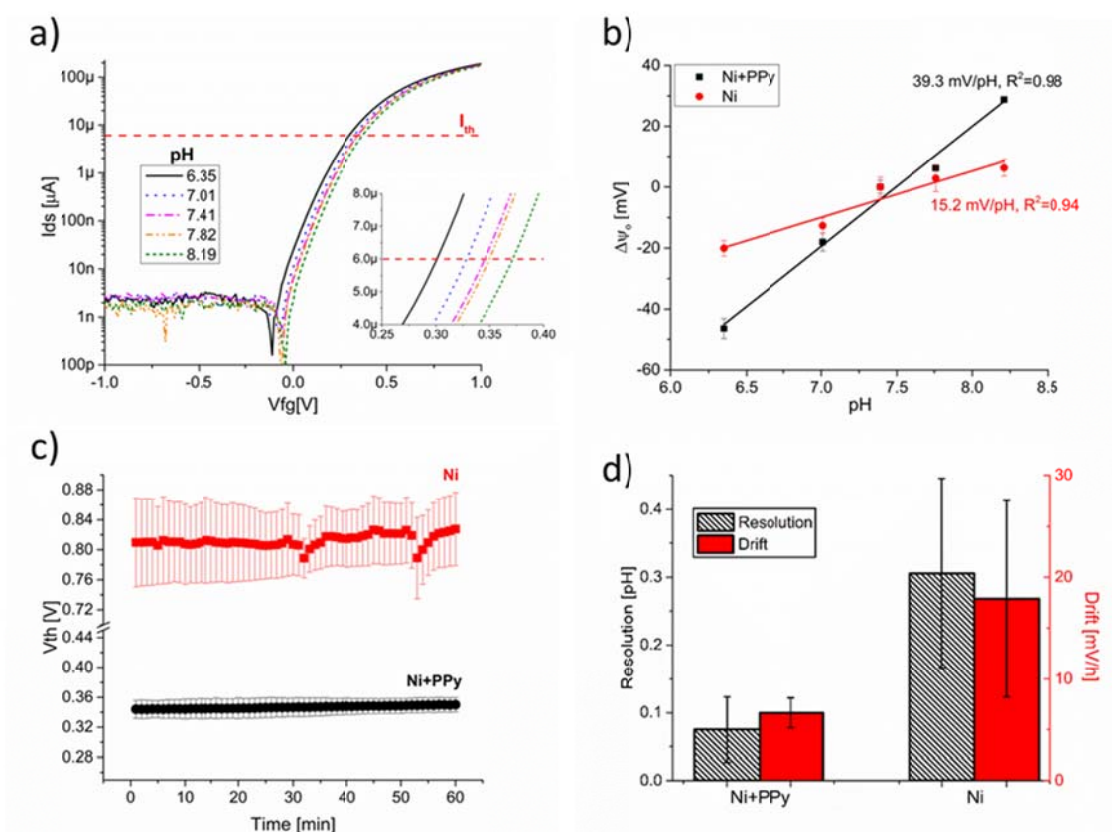


**Fig. 6** Assessment of ISFET operation with nickel-based electrodes. **(a)** pH dependent  $I_d$ - $V_g$  transfer curve of ISFET biased with a Ni+PPy electrode. The inset zooms in the area of threshold current that is used to extract change in surface potential. **(b)** Surface potential variation as a function of pH for transistors biased with bare Ni and Ni+PPy electrodes. **(c)** ISFET threshold voltage drift with Ni and Ni+PPy electrodes during a one hour experiment. **(d)** Comparison of pH resolution and threshold voltage drift of ISFETs biased with bare nickel and nickel + PPy electrodes.

The PPy electrodes are well-suited to be efficient on-chip quasi-reference electrodes for ISFET fabrication and operation. The stability and lack of pH response of the PPy electrodes is complemented with a simple and inexpensive manufacturing process. The electrodeposition

1  
2  
3  
4  
5  
6 method has several advantages when compared to other reported alternatives. First, it does not  
7  
8 require photolithography and etching steps that are used for other on-chip solid-state reference  
9  
10 electrodes. Second, the iteration of CV cycles assures that all the exposed metal will be covered by  
11  
12 the polymer, minimizing performance degradation caused by fabrication defects. Third, unlike  
13  
14 other processes that print electrodes, the polymerization of PPy can be easily scaled to create quasi-  
15  
16 reference microelectrodes in a parallel deposition process by setting up multiple nodes as the  
17  
18 working electrode. In addition, deposition of PPy does not involve chemical surface modifications  
19  
20 that may harm the FET's sensing hafnium oxide layer, and the materials required for the process  
21  
22 are inexpensive, especially when non-precious metals are used for patterning the microelectrode.  
23  
24 These advantages of the PPy electrodes make them good candidates for fabrication of ISFETs with  
25  
26 on-chip quasi-reference electrodes.  
27  
28

29  
30 The PPy electrodes will enable the use of ISFETS to perform and monitor biochemical reactions that  
31  
32 take place in small droplets, creating new opportunities for FET-based biological sensing. There are  
33  
34 several advantages for performing reactions in small volumes that can be exploited using the  
35  
36 microscopic ISFETs. Besides the obvious reduction of reagent consumption, performing reactions in  
37  
38 small volumes enables high-throughput screening assays, results in better sensitivity and  
39  
40 quantification, and permits fast and low energy thermo-cycling.<sup>46</sup> Therefore, the robust PPy  
41  
42 electrodes solve the issue of droplet electrolyte referencing. They will allow the integration of FETs  
43  
44 and droplet reactions creating a path for multiplexed, inexpensive, label-free, and portable  
45  
46 biological sensing.  
47  
48  
49  
50

#### 51 52 **4. Conclusions**

53  
54 In this paper, we presented a robust and low-cost method to create on-chip quasi-reference  
55  
56 electrodes for ISFET operation. Simple cyclic voltammetry deposition of polypyrrole on patterned  
57  
58 electrodes yielded robust quasi-reference electrodes that have stability and pH response similar to  
59  
60

1  
2  
3  
4  
5  
6 the conventional Ag/AgCl. We characterized the deposited polypyrrole film on the microelectrodes  
7  
8 by studying its deposition process and performing open circuit potential measurements to evaluate  
9  
10 its electrical performance. We showed the isotropic growth of micrometer polypyrrole layers on  
11  
12 the patterned microelectrodes and demonstrated that these quasi-reference electrodes are stable  
13  
14 within 1 mV, have a drift of only 1- 2 mV/h, and a present a low pH response of around 5 mV/pH.  
15  
16 These characteristics are substantially better than the ones obtained with bare metal electrodes  
17  
18 and translate into robust ISFET operation with close to Nernstian sensitivity and good pH  
19  
20 resolution. Furthermore, we polymerized PPy in different metals demonstrating that the technique  
21  
22 can be expanded to non-precious metals like nickel, showing a clear path for integration of these  
23  
24 quasi-reference electrodes to the semiconductor foundry fabrication processes.  
25  
26

27  
28 On-chip reference electrodes are smaller, more robust, less expensive, and simpler to package than  
29  
30 the common glass packed reference electrodes. The polypyrrole on-chip electrodes that we studied  
31  
32 have all those desirable characteristics with the added bonuses of simple fabrication, low cost, and  
33  
34 facile integration with other process of a semiconductor foundry. We believe that these new on-  
35  
36 chip electrodes will allow novel applications of ISFET sensing by enabling the use of smaller  
37  
38 electrolyte volumes and simplifying implementation of portable applications.  
39  
40  
41  
42  
43  
44  
45  
46  
47  
48  
49

#### 50 Acknowledgements

51  
52  
53 We acknowledge funding support from a cooperative agreement with Purdue University and the  
54  
55 Agricultural Research Service of the United States Department of Agriculture, project number 1935-  
56  
57 42000-035, and a sub-contract to the University of Illinois at Urbana-Champaign. In addition, we  
58  
59 acknowledge support from the Center for Innovative Instrumentation Technology (CiIT) of the  
60  
University of Illinois at Urbana-Champaign.

1  
2  
3  
4  
5  
6  
7 References  
8

- 9  
10  
11  
12  
13  
14  
15  
16  
17  
18  
19  
20  
21  
22  
23  
24  
25  
26  
27  
28  
29  
30  
31  
32  
33  
34  
35  
36  
37  
38  
39  
40  
41  
42  
43  
44  
45  
46  
47  
48  
49  
50  
51  
52  
53  
54  
55  
56  
57  
58  
59  
60
1. J. Lu and M. Bowles, *Qual. Assur. Saf. Crop. Foods*, 2014, **6**, 123–133.
  2. P. Vadgama, S. Anastasova and A. Spehar-Deleze, in *Detection Challenges in Clinical Diagnostics*, 2013, pp. 35–64.
  3. A. J. Baeumner, C. Jones, C. Y. Wong and A. Price, *Anal. Bioanal. Chem.*, 2004, **378**, 1587–1593.
  4. P. Yager, G. J. Domingo and J. Gerdes, *Annu. Rev. Biomed. Eng.*, 2008, **10**, 107–44.
  5. C. Guiducci and F. M. Spiga, *Nat. Methods*, 2013, **10**, 617–8.
  6. G.-J. Zhang and Y. Ning, *Anal. Chim. Acta*, 2012, **749**, 1–15.
  7. C. Toumazou and P. Georgiou, *Electron. Lett.*, 2011, **47**.
  8. D. G. Pijanowska and W. Torbicz, *Sensors Actuators B Chem.*, 1997, **44**, 370–376.
  9. A. Soldatkin, J. Montoriol, W. Sant, C. Martelet and N. Jaffrezic-Renault, *Talanta*, 2002, **58**, 351–357.
  10. K.-I. Chen, B.-R. Li and Y.-T. Chen, *Nano Today*, 2011, **6**, 131–154.
  11. C. Beadling, T. L. Neff, M. C. Heinrich, K. Rhodes, M. Thornton, J. Leamon, M. Andersen and C. L. Corless, *J. Mol. Diagn.*, 2013, **15**, 171–6.
  12. K. Lee, P. R. Nair, A. Scott, M. a Alam and D. B. Janes, *J. Appl. Phys.*, 2009, **105**, 102046.
  13. A. Michalska, *Electroanalysis*, 2012, **24**, 1253–1265.
  14. I.-Y. Huang and R.-S. Huang, *Thin Solid Films*, 2002, **406**, 255–261.
  15. M. W. Shinwari, D. Zhitomirsky, I. a Deen, P. R. Selvaganapathy, M. J. Deen and D. Landheer, *Sensors (Basel)*, 2010, **10**, 1679–715.
  16. I.-Y. Huang, S.-H. Wang, C.-C. Chu and C.-T. Chiu, *J. Micro/Nanolithography, MEMS, MOEMS*, 2009, **8**, 033050.
  17. B. J. Polk, A. Stelzenmuller, G. Mijares, W. MacCrehan and M. Gaitan, *Sensors Actuators B Chem.*, 2006, **114**, 239–247.

- 1  
2  
3  
4  
5  
6 18. E. S. McLamore, J. Shi, D. Jaroch, J. C. Claussen, a Uchida, Y. Jiang, W. Zhang, S. S. Donkin, M. K.  
7  
8 Banks, K. K. Buhman, D. Teegarden, J. L. Rickus and D. M. Porterfield, *Biosens. Bioelectron.*,  
9  
10 2011, **26**, 2237–45.  
11  
12 19. J. Noh, S. Park, H. Boo, H. C. Kim and T. D. Chung, *Lab Chip*, 2011, **11**, 664–71.  
13  
14 20. G. Inzelt, in *Handbook of Reference Electrodes*, eds. G. Inzelt, A. Lewenstam and F. Scholz,  
15  
16 Springer Berlin Heidelberg, Berlin, Heidelberg, 2013, pp. 331–332.  
17  
18 21. H. Yang, S. K. Kang, C. A. Choi, H. Kim, D.-H. Shin, Y. S. Kim and Y. T. Kim, *Lab Chip*, 2004, **4**,  
19  
20 42–6.  
21  
22 22. E. Salm, Y. Zhong, B. Reddy Jr, C. Duarte-Guevara, V. Swaminathan, Y.-S. Liu and R. Bashir,  
23  
24 *Anal. Chem.*, 2014, **86**, 6968–6975.  
25  
26 23. J. Ghilane, P. Hapiot and A. J. Bard, *Anal. Chem.*, 2006, **78**, 6868–72.  
27  
28 24. Y. Yoshida, S. Yamaguchi and K. Maeda, *Anal. Sci.*, 2010, **26**, 137–139.  
29  
30 25. D. Zhan, F. F. Fan and A. J. Bard, *Proc. Natl. Acad. Sci. U. S. A.*, 2008, **105**, 12118–22.  
31  
32 26. L. E. Barrosse-Antle, a. M. Bond, R. G. Compton, a. M. O'Mahony, E. I. Rogers and D. S.  
33  
34 Silvester, *Chem. - An Asian J.*, 2010, **5**, 202–230.  
35  
36 27. B. R. Dorvel, B. Reddy, J. Go, C. Duarte Guevara, E. Salm, M. A. Alam and R. Bashir, *ACS*  
37  
38 *Nano*, 2012, **6**, 6150–64.  
39  
40 28. C.-S. Lai, C.-M. Yang and T.-F. Lu, *Electrochem. Solid-State Lett.*, 2006, **9**, G90.  
41  
42 29. K. A. Yusof, S. H. Herman and W. F. H. Abdullah, in *IEEE International Conference on*  
43  
44 *Semiconductor Electronics (ICSE)*, 2014, pp. 491–494.  
45  
46 30. A. Ortiz-Conde, F. J. García Sánchez, J. J. Liou, A. Cerdeira, M. Estrada and Y. Yue,  
47  
48 *Microelectron. Reliab.*, 2002, **42**, 583–596.  
49  
50 31. M. Zhou, M. Pagels, B. Geschke and J. Heinze, *J. Phys. Chem. B*, 2002, **106**, 10065–10073.  
51  
52 32. D. Quéré, *Annu. Rev. Mater. Res.*, 2008, **38**, 71–99.  
53  
54  
55  
56  
57  
58  
59  
60

- 1  
2  
3  
4  
5  
6 33. H. Suzuki, H. Ozawa, S. Sasaki and I. Karube, *Sensors Actuators B Chem.*, 1998, **53**, 140–146.  
7  
8  
9 34. Y. Ma, S. Jiang, G. Jian, H. Tao, L. Yu, X. Wang, X. Wang, J. Zhu, Z. Hu and Y. Chen,  
10 *Energy Environ. Sci.*, 2009, **2**, 224.  
11  
12 35. C. Duarte-Guevara, F.-L. Lai, C.-W. Cheng, B. Reddy, E. Salm, V. Swaminathan, Y.-K. Tsui, H. C.  
13 Tuan, A. Kalnitsky, Y.-S. Liu and R. Bashir, *Anal. Chem.*, 2014, **86**, 8359–67.  
14  
15 36. X. Duan, Y. Li, N. K. Rajan, D. a Routenberg, Y. Modis and M. a Reed, *Nat. Nanotechnol.*, 2012,  
16 **7**, 401–7.  
17  
18 37. S. J. Slattery, J. K. Blaho, J. Lehnes and K. a. Goldsby, *Coord. Chem. Rev.*, 1998, **174**, 391–416.  
19  
20 38. A. Fog and R. P. Buck, *Sensors and Actuators*, 1984, **5**, 137–146.  
21  
22 39. L. Nyholm, *Analyst*, 2005, **130**, 599.  
23  
24 40. D. E. Tallman, C. Vang, G. G. Wallace and G. P. Bierwagen, *J. Electrochem. Soc.*, 2002, **149**,  
25 C173.  
26  
27 41. Y. Nishi, T. Sonehara, A. Hokazono, S. Kawanaka, S. Inaba and A. Kinoshita, in *Proceedings of*  
28 *2010 International Symposium on VLSI Technology, System and Application*, IEEE, 2010, vol.  
29 **15**, pp. 120–121.  
30  
31 42. B. Imbert, R. Pantel, S. Zoll, M. Gregoire, R. Beneyton, S. Del Medico and O. Thomas,  
32 *Microelectron. Eng.*, 2010, **87**, 245–248.  
33  
34 43. E. De Giglio, M. . Guascito, L. Sabbatini and G. Zambonin, *Biomaterials*, 2001, **22**, 2609–2616.  
35  
36 44. Y. Liu, Z. Liu, N. Lu, E. Preiss, S. Poyraz, M. J. Kim and X. Zhang, *Chem. Commun. (Camb)*,  
37 **2012**, **48**, 2621–3.  
38  
39 45. W.-Y. Chung, C.-H. Yang, D. G. Pijanowska, a. Krzyskow and W. Torbicz, *Electron. Lett.*, 2004,  
40 **40**, 1115.  
41  
42 46. E. Salm, C. Duarte-Guevara, P. Dak, B. R. Dorvel, B. Reddy, M. A. Alam and R. Bashir, *Proc.*  
43 *Natl. Acad. Sci. U. S. A.*, 2013, **110**, 3310–5.  
44  
45  
46  
47  
48  
49  
50  
51  
52  
53  
54  
55  
56  
57  
58  
59  
60

## Figure legends

**Fig. 1** Electrodeposition of PPy on on-chip patterned metal electrodes. **(a)** Schematic of the three-electrode cell used for deposition and schematic of the polymerization. The PDMS well is filled with the acetonitrile solution with pyrrole that gets polymerized during CV leaving a film of partially oxidized PPy on the microelectrode. **(b)** Typical deposition of PPy on platinum microelectrodes by CV, the peak currents increase in each cycle as the PPy electrode grows. **(c)** Image of independent on-chip platinum electrodes coated with the PPy layer. The edge of the PDMS well is clearly defined owing to the fact that only on-chip metal exposed to the acetonitrile solution is coated.

**Fig. 2** Characterization of the deposited PPy film. **(a)** Film thickness, **(b)** Profilometry total roughness (Rt), **(c)** Normalized area of the electrode, and **(d)** contact angle, as a function of the CV deposition cycles. **(e)** Optical image of square electrode array with different number of deposition cycles. **(f)** Scanning electron microscopy image of electrodes in the left side of the array presenting 0, 10, and 50 deposition cycles.

**Fig. 3** Open circuit potential (OCP) measurements of electrode stability and pH sensitivity in a 10mM KCl solution. **(a)** OCP vs. Ag/AgCl as a function of time for each electrode. The bands represent 3 experiments, having the thickness is correlated with repeatability, and fluctuations reflecting stability and drift. Comparative quantification of **(b)** stability and **(c)** drift of OCP measurements showing improved performance with PPy. **(d)** Measured OCP as a function of the electrolyte pH with the calculated linear regressions. **(e)** Extracted pH sensitivity for each electrode demonstrating reduced pH response of the PPy electrodes.

**Fig. 4** Polymerization of PPy on nickel electrodes and electrical performance evaluation. **(a)** CV deposition of PPy film on nickel microelectrodes. **(b)** Bands of OCP stability as a function of time for nickel with and without the PPy layer. **(c)** OCP vs. electrolyte pH to assess pH sensitivity of nickel and nickel+PPy electrodes. The results of the linear regressions are reported as sensitivity.

**Fig. 5** Evaluation of ISFET operation with PPy microelectrodes. **(a)** Image of an extended-gate ISFET surrounded by a platinum+PPy and bare platinum electrodes used for comparative measurements. **(b)** ISFET transfer characteristics with platinum, PPy, and Ag/AgCl fluid-biasing electrodes. Solid lines represent the first measurement and dotted lines last measurement in a one hour experiment. The inset zooms in the area for constant current threshold voltage calculation. **(c)** Quantification of threshold voltage drift with each electrode and plot of threshold voltage as a function of time during a one hour experiment. Error bars represent variation between different experiments **(d)** Real time surface potential variations due to pH changes. The spikes every 200s in the plot indicate injection of NaOH in the PDMS reservoir. **(e)** ISFET surface potential as a function of pH with linear regressions to quantify sensitivity. **(f)** Comparative results of pH sensitivity and resolution of the ISFET operation with each electrode.

**Fig. 6** Assessment of ISFET operation with nickel-based electrodes. **(a)** pH dependent Id-Vg transfer curve of ISFET biased with a Ni+PPy electrode. The inset zooms in the area of threshold current that is used to extract change in surface potential. **(b)** Surface potential variation as a function of pH for transistors biased with bare Ni and Ni+PPy electrodes. **(c)** ISFET threshold voltage drift with Ni and Ni+PPy electrodes during a one hour experiment. **(d)** Comparison of pH resolution and threshold voltage drift of ISFETs biased with bare nickel and nickel + PPy electrodes.

## Table legends

**Tab. 1** Summary of stability, repeatability, drift, and pH sensitivity of electrodes made with different metals and with/without the deposited PPy film.